VACUUM DRYING OF LAYERED INSULATION ON EHT EQUIPMENT

I. F. Pikus and L. A. Koshepavo

UDC 676.2.052.7

A study has been made of the effects of operating conditions and radial thickness in a multilayer specimen on the vacuum drying rate and instantaneous layerwise water distribution in cable-insulating paper.

Considerable importance attaches to research on heat and mass transfer in vacuum drying of the insulation in high-voltage equipment (power and metering transformers, high-voltage leads, etc.), since such treatment is a major step in the production of such equipment, although little research has been done on it. Measurements on the major trends in drying in high-voltage cellulose insulation are usually performed on multilayer models such as cylindrical specimens with water-impermeable ends, which may be made up from cable-insulating paper as commonly used in electrical engineering and which simulate the elements most difficult to dry in such equipment [1-4]. We have used models consisting of cable paper type K-120 of width 160 mm wound tightly onto metal rods of diameter 16 mm; the radial thicknesses were 10, 20, 30, and 40 mm. The ends of the rods and the free end of the strip were rendered impermeable with epoxide resin. The methods of measurement have been described in some detail [5]. The specimens were placed in the working chamber between two vertical metal screened heaters, which were heated themselves by infrared lamps type KI-220-1000. The temperature was monitored from thermocouples attached close to the surface of the specimen. The operating parameters in combined convective and radiative heat transfer were varied within the following limits: 110 to 150°C, pressure in the working chamber 0.01 to 10 mm Hg. The results were processed to give combined curves for the heating and drying, and also for the time course of the internal pressure at various radii (Fig. 1). The pressure transducers were surgical needles of diameter 1.2 mm, which were placed between the layers of paper via one of the sealed ends at various distances from the metal rod. These needles were connected by thin metal tubes to a thermostatic measuring system, which included mercury vacuum gauges and type MT-6 transducers, which worked in conjunction with a VSB-1 vacuum gauge.

We used a linear relationship between the relative reduced drying rate $dW/d\tau/N(W - W_e)$ and the current excess mean water content of the paper [6], which is characteristic of this process and has been confirmed by experiment, and which gives generalized curves for the vacuum drying of such specimens:

$$-\frac{dW/d\tau}{N(W-W_e)} = a + b(W - W_e) \tag{1}$$

or

$$\tau = \frac{1}{aN} \ln \frac{[a + b(W - W_e)](W_1 - W_e)}{[a + b(W_1 - W_e)](W - W_e)}, \tag{2}$$

where a and b are empirical coefficients independent of the water content, operating parameters, and radial thickness; the values of these for all the specimens were derived from the data as $a = 0.013$ and $b = 0.019$.

The $N = f(t, P, h)$ functional relationship was derived (Figs. 2-4) for qualitative and quantitative analysis of the effects of major working parameters and insulation thickness on the performance.

Lykov Institute of Heat and Mass Transfer, Academy of Sciences of the Belorussian SSR, Minsk. Translated from Inzhenerno-Fizicheskii Zhurnal, Vol. 30, No. 1, pp. 139-146, January, 1976. Original article submitted January 23, 1975.

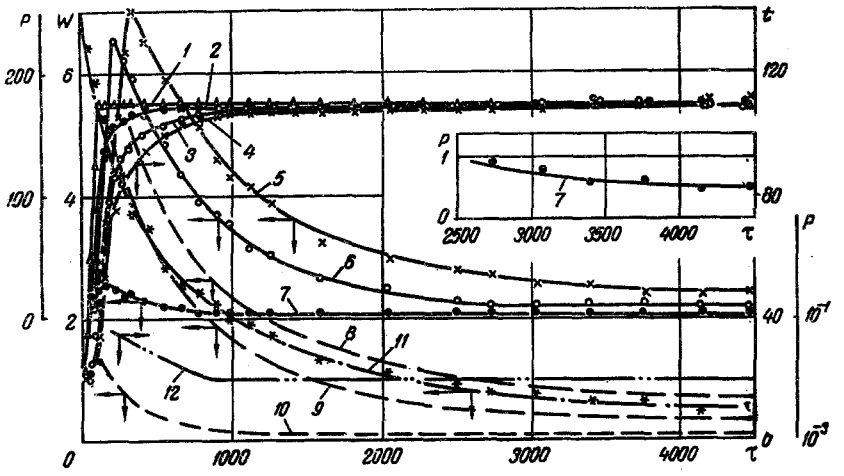

Fig. 1. Drying curves for a model specimen with h = 30 mm and local pressure, layer water content, and insulation temperature at t = 110°C and P = $1 \cdot 10^{-2}$ mm Hg: 1-4) temperatures of medium, surface layers, layers 20 mm from rod (middle layers), and internal layers, respectively; 5-7) pressures in internal, middle, and surface layers of insulation; 8-10) water contents of internal, middle, and surface layers; 11) drying curve for model specimen; 12) pressure in working chamber. τ in min, P in mm Hg, t in °C, and W in %.

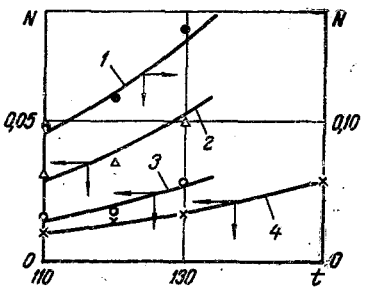

Fig. 2. Curves for N = f(t) for P = $1 \cdot 10^{-2}$ mm Hg for model specimens of thicknesses h (mm) of: 1) 10; 2) 20; 3) 30; 4) 40. N in %/min, t in °C.

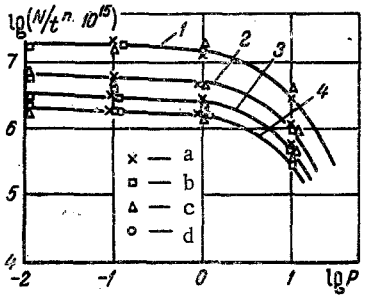

Fig. 3. Curves for log (N/t^n) = f·(log P): 1) h = 10 mm; 2) 20; 3) 30; 4) 40; a) t = 110°C; b) 120°C; c) 130°C; d) 150°C.

The temperature dependence of the maximum drying rate (Fig. 2) was of the same type for all specimens and of the form

$$N \sim t^n, \tag{3}$$

where the value of n is governed by the pressure in the working chamber, and is described as follows for the entire range in P:

$$n = 2.4 \lg (P + 23). \tag{4}$$

The residual pressure in the working chamber affects not only the drying rate as a function of temperature, but also the evaporation rate and the modes of heat and mass transfer within the insulation.

The rate of high-speed drying in such a multilayer system of cellulose under vacuum is governed in the main by the migration of water vapor under the pressure gradient. The vapor passing through the material has to overcome a constantly increasing diffusion resistance (increasing on account of the increased thickness of the dry layer, and also because of shrinkage). The mode of flow of the vapor is dependent on the working pressure and is governed by

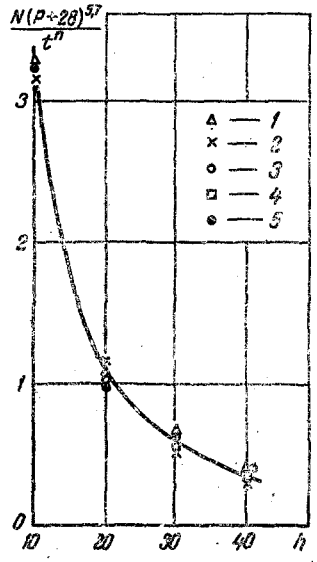

Fig. 4. Curve for $N(P + 28)^{5.7}/t^n = f(h)$: 1) t = 110°C, P = 1 mm Hg; 2) 120°C and 10; 3) 130 and P = 10; 4) 150 and $P = 1 \cdot 10^{-1}$; 5) t = 120°C, $P = 1 \cdot 10^{-2}$ mm Hg. h in mm.

the relationship between the mean free path of the vapor molecules and the size of the pores in the material. The pores in the fibrous cellulose material can be considered as a system of connected capillaries of equivalent diameter 10^{-6}-10^{-7} [7, 8]. The molecular mean free path is inversely proportional to P. At low pressures, the pore size in the insulation becomes less than the mean free path, and then the molecular mode of flow sets in, in which the flux density under isothermal conditions is described approximately by the following [9]:

$$j = 1.064 \sqrt{\frac{M}{RT}} r \frac{dP}{dh}. \qquad (5)$$

This implies that there exists a certain P below which a reduction by more than an order of magnitude relative to the pressure within the specimen should not produce a marked increase in the internal mass-transfer rate. The movement of the water vapor can be accelerated substantially under these conditions only by raising the vapor pressure within the insulation by raising the temperature. In that case, the fall in $1/\sqrt{T}$ [7] is of secondary importance, since the rise in the vapor pressure with temperature is far greater than the fall in $1/\sqrt{T}$ in (5). For instance, the sorption isotherms for cable paper [10] for a water content of 1% indicate that raising the temperature from 100 to 120°C under conditions of hydrothermal equilibrium can increase the partial pressure of the water vapor over the material from 25 to 60 mm Hg (i.e., by a factor 2.4), whereas $1/\sqrt{T}$ falls only by a factor 1.03; then it has been concluded [11] that the rate of a process cannot be increased substantially by reducing the external pressure if the internal mass transport in the insulation is by molecular diffusion.

However, in quantitative evaluation of the drying rate in relation to pressure one needs to incorporate the change in the equilibrium water content of the paper in accordance with (1), and this falls as P is reduced. Particular attention has been given to this previously [7], where it was considered that drying under vacuum for comparatively thick specimens causes the rate of internal vapor diffusion to be dependent on the difference in water contents between the internal and outer layers; the water content of the surface layers (particularly at the end) is governed by the conditions in the external medium, including the pressure in the drying chamber. Therefore, these trends in vacuum drying for comparatively thick porous materials would appear to apply only for reasonably high excess water contents, when the pressure within the specimen exceeds the vapor pressure in the external medium by more than an order of magnitude. In that case, if the drying is continued down to very low residual water contents, the pressure within the specimen in the latter stages may be comparable with the pressure in the working chamber; in that case, the chamber pressure may have an appreciable effect on the drying rate, which ultimately may affect the overall time required. Even an approximate consideration shows that a reduction in We as a result of reducing the vapor pressure in the surroundings can substantially accelerate the drying when the residual water content has become low, and thus one is completely justified in reducing the pressure at the end of drying for multilayer specimens.

Of course, in discussing the effects of pressure on the drying rate one has to consider how the permeability of the cable paper is dependent on P.

Measurements [4] on kraft paper of various densities and thicknesses (ρ = 0.67-1.08 g/cm^3, h = 70-125 μm) have shown that the permeability factor is virtually independent of P at the low pressures corresponding to the molecular mode of flow (P < 10-20 mm Hg).

All these features of the internal transport are reflected in our results; Fig. 3 shows log (N/t^n) = f(log P), which indicates that reducing the residual pressure in the chamber (in the working range of P) at first causes the reduced drying rate (N/t^n) to increase, but that the value stabilizes in the region of P = 1 mm Hg, in spite of further reduction in the external pressure. These curves are closely described by the following empirical relation:

$$\frac{N}{t^n} = \frac{C}{(P+28)^{5.7}}, \tag{6}$$

where C is dependent on the radial thickness; this is shown in Fig. 4 and can be put as follows:

$$C = \frac{130}{h^{1.6}}. \tag{7}$$

We thus have the following equation derived from (2) on the basis of the numerical values for the coefficients, which gives the drying time needed for cylindrical multilayer specimens made of cable paper:

$$\tau = \frac{0.59h^{1.6}(P+28)^{5.7}}{t^{2.41g(P+23)}} \ln \frac{[1+1.46(W-W_e)](W_1-W_e)}{[1+1.46(W_1-W_e)](W-W_e)}. \tag{8}$$

There is not more than 10-15% discrepancy between the curves constructed from (8) and recordings made in the above parameter ranges.

Experience shows that the pressure in all layers of the specimen rises to some definite maximum value P_{max} in the initial stage, in spite of the rapid fall in the residual pressure in the chamber, which is due to rapid bulk evaporation of the water and the comparatively high resistance of the internal layers. The time needed to reach P_{max} and the value of the latter corresponding to the singular point on the P = f(τ) curve are dependent on the point at which the pressure is measured: the minimum value for P_{max} and the least time to attain this τ_{max} are found for the surface layers, while the largest values correspond to the deepest layers. When the maximum has been passed, the pressure falls smoothly in all layers and tends exponentially to the pressure in the working chamber. At the end of the run, the pressure in the surface layers becomes virtually equal to the external pressure. The pressures in the internal and middle layers vary in the same general way, and at the end, when the mean water content of the specimen has fallen to about 0.5=0.6%, the pressure begins to fall more slowly. In all cases, the residual pressure in the internal layers remains fairly substantial even after the drying curve appears to have stabilized and may be in the range 5-30 mm Hg, the exact value being dependent on the working parameters, specimen thickness, and run time.

The pressure difference across the insulation thickness also varies substantially during the run, and this is one of the major factors affecting the internal mass transport. For instance, for the run shown in Fig. 1 the value of $\Delta P = p^{int} - p^{sur}$ at first rose from 0 to 230 mm Hg (the latter value corresponded to τ = 250 min), and then fell gradually to the final value of ΔP = 22 mm Hg (at τ = 4480 min). This highly nonstationary pressure distribution goes with a very substantial and continuously varying pressure gradient, so it is likely that all possible types of vapor transport will occur, from filtration to molecular or diffusion type.

The effects of the working conditions on the internal pressure indicate that the decisive effect on the internal transport under otherwise equal conditions comes from the operating temperature in conjunction with the radial thickness. As the temperature is raised, the pressure rise in all layers is accelerated, and when the maximum is passed there is a more rapid fall in the internal pressure. Any increase in the radial thickness with unchanged working conditions raises the pressure in the inner layers, while the rate of fall in P on the

descending branches of $P = f(\tau)$ is reduced. Further, on increasing h the ranges of apparent stabilization in the inner layers shift to larger times. The final values for the residual internal pressures in the inner layers of thick specimens are higher for comparable drying times and other operating conditions. Even a reduction in the residual chamber pressure by two orders of magnitude (from 1 to 10^{-2} mm Hg) did not alter the shape of the $P = f(\tau)$ curves substantially, nor did it affect the pressures in the middle and internal layers.

These results were used in quantitative evaluation of the layerwise distribution of the water and the rate of drying; it was assumed that the pressure in any layer was equal to the partial pressure of the water vapor and further that this partial pressure corresponded to equilibrium under the working conditions (temperature and water content) in the measurement zone [2, 4]. The current local water content was calculated from the empirical relation for the equilibrium water content for paper type K-120 as a function of temperature and vapor pressure under vacuum conditions [10]:

$$W_e = 6.1 \exp(-0.04t)\, P^{0,33(1+0,01t)} \qquad (9)$$

The current values for the local temperatures in each of the zones were taken from the curves for the surface, middle, and internal layers as recorded during the kinetic studies.

The broken lines in Fig. 1 show the calculated curves for the layerwise water contents for cellulose.

These drying curves are not only similar to the drying curve for the specimen as a whole, but also show that the time course of the mean water content lies in a region bounded by the limiting curves representing the drying of the outermost and innermost layers. These results are confirmed by direct measurement of the water content on paper from various layers in the specimen as determined by Fisher's method (these analyses were performed on small specimens taken after the run by means of a special sampler from the three zones indicated above). For instance, in a run with a specimen having h = 30 mm at 120°C and P = 1 mm Hg, the water contents of the layers after drying for 53 h as calculated from the curves were $W_{sur} = 0.1\%$, $W_{mi} = 0.5\%$, $W_{in} = 0.74\%$; the corresponding values from direct analysis were 0.24, 0.74, and 0.72%. This shows that the method is satisfactory and provides scope for qualitative and quantitative analysis of the water distribution during vacuum drying in high-voltage cellulose insulation, and that measurements on the internal pressure and temperature can be employed for the purpose.

NOTATION

W, W_1, W_e, instantaneous, initial, and equilibrium water contents, respectively, %; τ, time, min; $dW/d\tau$, drying rate, %/min; N, maximum drying rate for initial water content of the material, %/min; t, T, temperature, °C and °K, respectively; P, pressure, mm Hg; h, thickness of model sample, mm; r, radius of microcapillary, cm; M, molecular weight of water vapor; R, universal gas constant; α, b,C, empirical coefficients. Indices: sur, mi, in, surface, middle, and internal insulation layers in a model sample, respectively.

LITERATURE CITED

1. S. D. Lizunov, Drying and Outgassing for High-Tension Transformer Insulation [in Russian] Énergiya, Moscow (1971).
2. H. Bijr et al., "Transformers," in: Translations and Abstracts of Papers at CIGRE [in Russian], Énergiya, Moscow (1968).
3. A. Csernatony-Hoffer, IEEE Trans. Elec. Insul., EI-3, No. 4, 97-105 (1968).
4. Terada Tetsuro and Enokubo Fimiaki, Japan Elec. Eng. Inst., 92-A, 5, 207-213 (1972).
5. I. F. Pikus, L. A. Koshepavo, and A. V. Gudko, in: Thermophysics and Technology of Thermal Drying Processes [in Russian], ITMO AN BelorusSSR, Minsk (1975).
6. I. F. Pikus, L. S. Gimpeleva, and L. A. Koshepavo, Inzh.-Fiz. Zh., 22, No. 3 (1972).
7. M. Beyer, Grundlagen der Vakuumtrocknung von Flussigen Isolierstoffen und Papierisolation, DBR (1966).
8. H. Corte, Das Papier, 7 (1965).
9. A. V. Lykov, Theory of Drying [in Russian], Énergiya, Moscow (1968).
10. P. S. Kuts, I. F. Pikus, and L. S. Kalinina, in: Heat and Mass Transfer, Vol. 6 [in Russian], ITMO AN BelorusSSR, Minsk (1972).
11. I. Laszlo, Elektrotechnika, 61, 10-11, 393-401 (1968).